

# Momentum-Based Reactive Stepping Controller on Level and Non-level Ground for Humanoid Robot Push Recovery

Seung-kook Yun and Ambarish Goswami

**Abstract**—This paper presents a momentum-based reactive stepping controller for humanoid robot push recovery. By properly regulating combinations of linear and angular momenta, the controller can selectively encourage the robot to recover its balance with or without taking a step. A reference stepping location is computed by modeling the humanoid as a passive rimless wheel with two spokes such that stepping on the location leads to a complete stop of the wheel at the vertically upright position. In contrast to most reference points for stepping based on pendulum models such as the *capture point*, our reference point exists on both level and non-level grounds. Moreover, in contrast with continuously evolving step locations, our step location is stationary. The computation of the location of the reference point also generates the duration of step which can be used for designing a stepping trajectory. Momentum-based stepping for push recovery is implemented in simulations of a full size humanoid on 3D non-level ground.

## I. INTRODUCTION

For humanoid robots to exit from lab environments and to enter the real world where they can live together with humans, the ability of recovering from unexpected external disturbances such as a push is essential. The response of a humanoid robot to progressively increasing disturbances can be categorized into three situations: (1) postural balance control, (2) push recovery through reactive stepping, and (3) fall control. Reactive stepping differs from preplanned gait step in that it is a balance maintenance mechanism in response to a disturbance. This paper explores a unified strategy of postural balance control and reactive stepping integrated to the momentum controller proposed in [1].

For traditional balance controllers ([2], [3]), the focus has been primarily on linear momentum which is a scaled version of the CoM velocity. As attention has been given to angular momentum and the important role it plays in balance ([4], [5], [6]), the presented controller enables us to control both the angular momentum and linear momentum of a humanoid. Our balance controller in [1] attempted to attain the desired linear momentum at the cost of sacrificing precise control of the angular momentum. This encourages the robot to maintain balance by making postural adjustments without stepping (See Fig. 1(a)). In this paper we show the opposite approach (See Fig. 1(b)) in which the controller prioritizes angular momentum over linear momentum. Combined with a stepping controller for the swing leg, this leads to a natural looking reactive stepping such that a humanoid can recover from a strong push by taking a step.

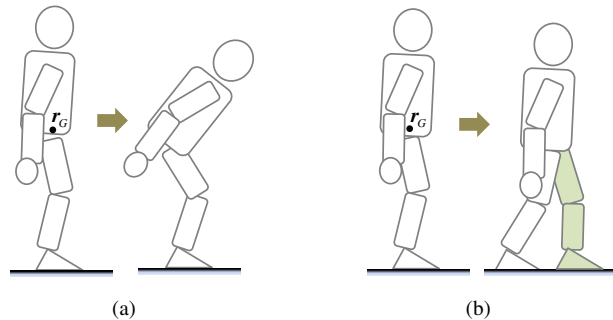


Fig. 1. In momentum control, when the ground reaction force and the center of pressure computed from desired momentum rate change are not simultaneously achievable, two distinct scenarios can arise. (a) Fully respecting the desired linear momentum while compromising angular momentum (if needed) results in a postural balance control without stepping. (b) Contrarily, fully respecting the desired angular momentum while compromising linear momentum (if needed) results in a stepping motion.

When a robot is under external disturbance, finding an appropriate stepping location for balance recovery is important to minimize control effort. For instance, a stepping controller should attenuate the extra momentum created by an external push as well as follow a stepping trajectory of the swing leg. If we carefully choose the stepping location, the controller may use most of its effort for stepping while the attenuation of the momentum can be achieved almost passively.

We propose the *generalized foot placement estimator* (GFPE) as a reference point for stepping on level and non-level ground by modeling the robot as a rimless wheel with two spokes as shown in Fig. 2. On flat ground, the GFPE coincides with the foot placement estimator (FPE) introduced in [7]. The GFPE is chosen so that the center of mass (CoM) will stop vertically upright over the stepping location after the robot takes a step. In theory, this process is completely passive without any actuation or control. In practice, the robot is controlled such that the swing leg steps at the chosen point, and the discrepancy due to the difference between the rimless wheel model and the actual humanoid such as the dynamic effect of swing leg motion is compensated by the controller.

Another benefit is that the introduced GFPE has predictive property. Most reference points for stepping (reactive or preplanned gait) such as the *capture point* ([8]) and *extrapolated center of mass* ([9]) should be instantaneously stepped at when they are computed, and they continue to evolve over time [10]. However, the computation of the GFPE automatically calculates a duration of stepping during which the rimless wheel rotates and the GFPE remain stationary

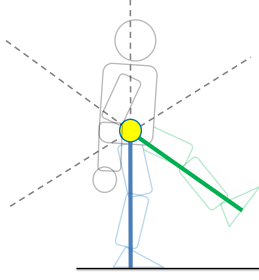


Fig. 2. A planar rimless wheel model with only two spokes is superposed on a humanoid robot. The model has a point mass at the center which corresponds to the CoM of the robot. The spokes are massless, have a fixed length and correspond to the legs of the robot. The gray dashed spokes are omitted and only two spokes, corresponding to the two robot legs, are actually used.

until the swing spoke touches the ground. This duration of stepping can be used to design trajectories of the CoM and the swing leg.

Our current work is similar to [11] and [7] although it is more general and can be applied on both level and non-level grounds. The previous works have not paid much attention on how to choose an *anchor point* which the simplified models (linear or non-linear inverted pendulums) rotate about. Note that the feet of a humanoid have non-zero contact area while the pendulum models have a point contact. It turns out that the choice of the anchor point can significantly change the GFPE. We propose how to select a plane on which the simplified humanoid model resides and an anchor point. We also prove the uniqueness of the GFPE.

The momentum-based stepping controller on non-level ground has been implemented to perform reactive stepping on 3D non-level ground with various magnitude and direction of pushes in the Webots simulator [12].

## II. STEPPING USING MOMENTUM CONTROLLER

Our previous work [1] presented a balance strategy for a humanoid robot which controls both the linear and angular momentum of the robot. This work focused on purely postural balance recovery which does not require stepping. The balance controller controls rate changes of linear and angular momenta according to the following rules:

$$\dot{\mathbf{k}}_d = \Gamma_{11}(\mathbf{k}_d - \mathbf{k}) \quad (1)$$

$$\dot{\mathbf{l}}_d/m = \Gamma_{21}(\dot{\mathbf{r}}_{G,d} - \dot{\mathbf{r}}_G) + \Gamma_{22}(\mathbf{r}_{G,d} - \mathbf{r}_G) \quad (2)$$

where  $\mathbf{k}$  and  $\dot{\mathbf{k}}$  are centroidal angular momentum and its rate change,  $m$  is the total mass of the robot,  $\mathbf{r}_G$  and  $\dot{\mathbf{r}}_G$  are the locations and the velocity of the CoM.  $\mathbf{k}_d$  and  $\dot{\mathbf{l}}_d$  are the *desired* rates of change of centroidal angular and linear momenta<sup>1</sup>, respectively, and  $\mathbf{r}_{G,d}$  is the desired CoM position.  $\Gamma_{ij}$  represents a  $3 \times 3$  diagonal matrix of feedback gain parameters. The momentum controller checks if the desired momentum rates are *admissible*, which are defined as physically realizable, and optimizes joint torque according to the admissible momentum. The details can be found in [1].

<sup>1</sup> $\dot{\mathbf{k}}_d$  and  $\dot{\mathbf{l}}_d$  are *not* derivatives of  $\mathbf{k}_d$  and  $\mathbf{l}_d$

In order to provide maximum ability to the postural balance controller such that the robot can withstand forces without requiring to take a step, the controller respects linear momentum in preference to angular momentum. With the proposed controller a biped robot can recover balance from an external push by generating angular momentum, if necessary, as shown in Fig. 1(a). However, when a push is so large that a robot cannot recover balance solely by postural movement, taking a step becomes inevitable as shown in Fig. 1(b).

In this paper, we formulate and integrate a step controller to the existing momentum based balance controller, which is applicable for both level and non-level grounds. The balance controller and the step controller are managed by a high level controller which makes the decision to trigger the step controller.

The integration of the step controller and the balance controller is enabled by the key observation that different choices of the gain matrices yield different push recovery behaviors. For example, a small  $\Gamma_{11}$  and a large  $\Gamma_{21}, \Gamma_{22}$  will generate the motion shown in Fig. 1(a) after a push from behind. Normally the desired angular momentum is set to zero to keep the robot upright, and the bending motion such as Fig. 1(a) generates angular momentum which contributes to the error in  $\dot{\mathbf{k}}$ . However, the generated angular momentum helps to pull the CoM backward and the small  $\Gamma_{11}$  makes the controller almost ignore the angular momentum error. On the other hand, a large  $\Gamma_{11}$  causes the robot to respect angular momentum more strictly. When the desired angular momentum is zero, which is reasonable for stepping motion, the controller would move the robot CoM position rather than bend the upper body. The robot generates linear momentum which causes error for  $\dot{\mathbf{l}}$ , however the error is scaled down because of the small  $\Gamma_{21}$  and  $\Gamma_{22}$ , and the robot controller prioritizes the desired angular momentum over the desired linear momentum. By adding a low-level stepping controller to this momentum controller, reactive stepping may be achieved as shown in Fig. 1(b).

The low-level controller outputs a target step point, GFPE, calculated from the rimless wheel model, and trajectories of the CoM and the swing foot of the robot. Now we describe the details of the reactive stepping controller.

## III. GENERALIZED FOOT PLACEMENT ESTIMATOR ON NON-LEVEL GROUND

Our reactive stepping controller is based on a simplified dynamic model of the humanoid: a rimless wheel with only two spokes (See Fig. 2). We assume that the rimless wheel model has massless spokes and a point mass at the center of the wheel. The central idea behind the controller is as follows: when the high level controller decides to execute a step due to a large push, the reactive stepping controller computes the stepping location where the rimless wheel model would come to a complete stop with its CoM directly above the step location as shown in Fig. 3(c). We call this stepping point the *generalized foot placement estimator* (GFPE). This is an extension of the FPE [7]. Note that we

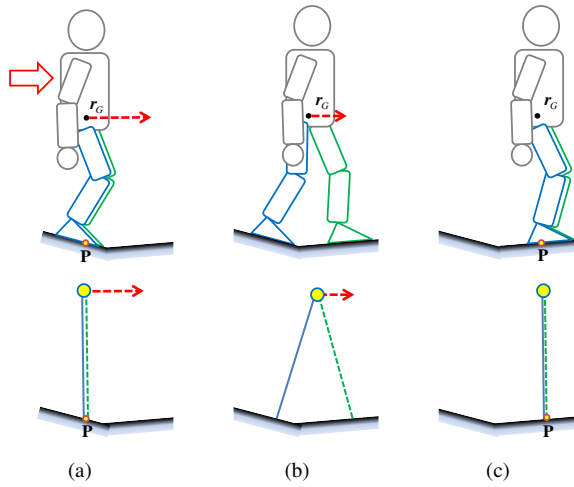


Fig. 3. Reactive stepping of a humanoid after a push from behind (top row) and its rimless wheel model (bottom row).  $r_G$  is the CoM location and  $p$  is the CoP location of the robot. The two legs (spokes) are depicted by solid blue and dotted green respectively. The dotted red arrow indicates the velocity of the CoM. (a) The humanoid is subjected to a push from behind. (b) The humanoid takes a step on the second slope. (c) A follow-up step is executed to bring the robot to a vertically upright position.

first compute the GFPE and the corresponding configuration of the rimless wheel will be created with its *leg angle*  $\alpha$  defined as the half of the angle between the two spokes (See Fig. 6), which is computed according to the GFPE.

Since the rimless wheel model is defined in 2D and the robot exists in 3D, we determine a plane on which the simplified rimless model resides. We assume that the robot will move in the same direction as the velocity of the robot CoM,  $\dot{r}_G$ , just after a push. Consequently, the GFPE will be located on the line of  $\dot{r}_G$  projection on the ground. As shown in Fig. 4, the 2D plane for the rimless wheel is defined by two vectors:  $\dot{r}_G$  and the vertical through the CoM. Note that the magnitude and direction of the push are not required. The selected plane is solely dependent on the states of the robot after the push.

Upon the 2D plane, we define an *anchor point* where the rimless wheel touches the ground and rotates about. Setting the anchor point is important since the robot has extended feet while the rimless wheel model has a point contact. Furthermore, the location of the anchor point determines the GFPE location and even the decision for taking a step. The previous works which used the FPE [11], [13] did not explicitly explain this choice of this point. They seemed to use the ground projection of the CoM, or the feet of their robot actually had a point contact. However, if we set the projected CoM as the anchor point, even a small push may result in a big step which may not be necessary at all. For instance, let a humanoid pushed from behind as in Fig. 4. If the anchor point ( $P$  in Fig. 4) is ahead of the projected CoM, the kinetic energy from a small push would be dissipated before the CoM rotates and passes over the vertical line through the anchor point, which implies no step is necessary since the robot would not topple forward from that small push. In contrast, if we use the projected CoM as the anchor

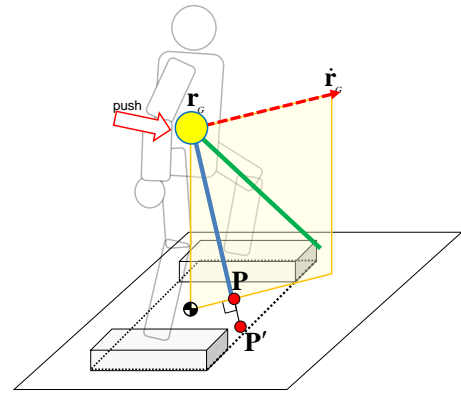


Fig. 4. A 2D plane on which the rimless wheel model is defined. The plane is determined by two vectors: the vertical through the CoM and the velocity  $\dot{r}_G$  of the CoM.  $P'$  is the actual CoP of the robot and  $P$  is the *projected* CoP located on the wheel plane about which the wheel rotates. The region enclosed by the dotted black lines is the support convex hull for the robot. The two feet of the robot are exaggerated to clearly show the convex hull and the points.

point, the same push will make the CoM of the rimless wheel pass over the vertical, which would imply that the robot would topple forward and stepping would become necessary.

In this work, we use *projected* CoP  $P$  as the anchor point, as shown in Fig. 4. We project the CoP  $P'$  of the robot on the 2D plane and assume that the rimless wheel rotates about the projected CoP,  $P$ . From now on,  $P$  represents the projected CoP. Note that the CoP reacts to a push much faster than the CoM since it depends on CoM acceleration. For example, just after a push from behind, the CoP will be ahead of the CoM as in Fig 4.

Assuming that the robot knows the ground slopes, this GFPE exists in most cases unless stepping is physically not feasible due to the fixed length of the spokes or a steep slope (discussed in Section III-C). Note that most of the ground reference points for stepping such as FPE, ZMP [14], FRI [15] and capture point [8] are defined only on the flat ground.

One can envision a number of initial scenarios of push recovery after a push from behind, and the most probable one is shown in Fig. 5 where the robot is standing still and is subjected to a push from behind. The CoM will lag behind the CoP when the push is from behind. In this paper we will primarily focus on this scenario and the developed controller can be adapted to the other scenarios with ease.

Next we introduce the dynamics of the rimless wheel model and derive the GFPE for reactive stepping on non-level ground.

#### A. Dynamics of rimless wheel model

We start with a brief review of the dynamics of the rimless wheel model. The model has a point mass at the center, rotational inertia about the anchor point, and massless spokes. To match this model to a biped robot, the center location of the rimless wheel is chosen as the CoM of the robot and only two spokes are used for the two legs of the robot. The rotational inertia of the model is equal to the

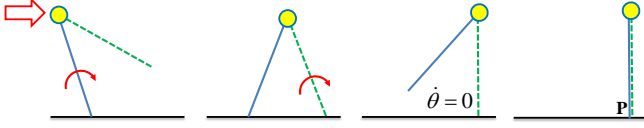


Fig. 5. Most probable scenario of reactive stepping following a push based on the rimless wheel model on level ground.  $\theta$  is the angular velocity of the support spoke. The scenario has four phases. In the first phase, the CoM is behind the anchor point, however it will pass over the anchor point since the robot has enough kinetic energy. The rimless wheel takes a step at the second phase and stops with the CoM above the foot contact at the end of the third phase. The first and third phases can be seen as an inverted pendulum model, and the second phase is the instantaneous phase of collision where the wheel loses energy. The last phase is a follow-up step which makes the swing spoke (blue solid line) take a step at the same step location of the support spoke (dotted green line).

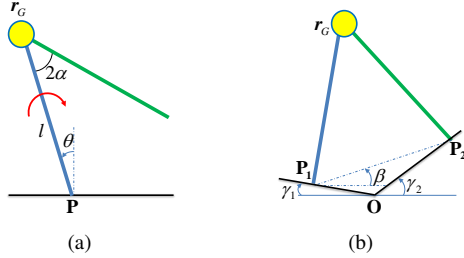


Fig. 6. Two-spoke rimless wheel model of a biped. (a) Single contact phase:  $l$  is spoke length,  $P$  is the projected CoP about which the biped is rotating,  $\theta$  is the angle made by the support spoke with the vertical and  $\alpha$ , called the leg angle, is the half of the angle between the spokes. (b) Double contact phase:  $P_1$  and  $P_2$  are the two contact points.  $\gamma_1$  and  $\gamma_2$  are the slope angles.  $O$  is the point of intersection of the slopes, and  $\beta$  is the angle made by  $P_1P_2$  with the horizontal.

rotational inertia of the robot about  $P$ . More details of the model can be found in [16]. For discussion of the model we assume a flat ground, however our stepping strategy is valid for general non-level ground.

We review the dynamic equations for each of the four phases in the scenario of Fig. 5. The equation of motion for a rimless wheel is that of an inverted pendulum when it is in the single contact phase (first and third phases), shown in Fig. 6(a).

$$I_P \ddot{\theta} = mgl \sin \theta, \quad (3)$$

where  $\theta$  is the angle made by the support spoke and the vertical as shown in Fig. 6(a),  $I_P$  is the rotational inertia of the rimless wheel about  $P$ ,  $m$  is mass, and  $g$  is the acceleration due to gravity. Until stepping of the swing leg, the total mechanical energy of the rimless wheel  $E$  is conserved.

At time  $t^-$  just before the touchdown collision, the conservation of  $E$  leads to the following relationship:

$$\dot{\theta}(t^-) = \pm \sqrt{\frac{2}{I_P} (E - mgl \cos \alpha)}, \quad (4)$$

since  $\theta(t^-) = \alpha$ . The sign of  $\dot{\theta}(t^-)$  is decided by the initial condition. For example, in the convention of Fig. 6(a), the sign is negative.

During the collision in the second phase, we assume that the angular momentum of the model,  $k_P$ , is conserved

around the collision point. In other words,

$$k_P(t^-) = k_P(t^+), \quad (5)$$

where  $t^+$  is the time just after the collision. The collision results in an instantaneous loss of angular velocity given by:

$$\dot{\theta}(t^+) = \dot{\theta}(t^-) \cos(2\alpha). \quad (6)$$

Based on this dynamic model, we next determine the GFPE for reactive stepping on non-level ground.

### B. Whether to step on the next slope

On non-level ground with discrete slope change as shown in Fig. 6(b), the robot must decide if it should take a step on the first slope or the second slope. Introducing the constants  $d_1 = P_1O$  and  $d_2 = OP_2$ , where  $O$  is the point of intersection of the slopes,  $P_1$  is the anchor point and  $P_2$  is the touch-down location of the swing spoke on the second slope, the leg angle  $\alpha_o$  for stepping on  $O$  is determined as follows:

$$2l \sin \alpha_o = d_1. \quad (7)$$

The robot should take a step on the second slope if any of the two following conditions are satisfied:

- 1) After the step at time  $t^+$ , when the pivoting spoke just detached from the first slope,  $\theta(t^+) = \alpha - \gamma_1$  is negative. This means that the CoM has already crossed the vertical line through  $O$ .
- 2) Upon stepping at  $O$ , the kinetic energy is large enough for the robot to topple forward.

The first condition is purely geometric and it implies that

$$\gamma_1 > \alpha_o. \quad (8)$$

When  $\gamma_1 < \alpha_o$ , we need to look into the second condition: whether  $\dot{\theta}(0)$  is large enough for toppling. To satisfy the condition:

$$\dot{\theta}(0) > \sqrt{\frac{2mgl}{I_P} \left[ \cos(\alpha + \gamma_1) - \cos \theta(0) + \frac{1 - \cos(\alpha - \gamma_1)}{\cos^2(2\alpha)} \right]}. \quad (9)$$

Eqs. 8 and 9 together are the conditions for the robot to take a step on the second slope. Next we proceed to determine where to step on the second slope if the sufficient conditions are met.

### C. Where to step

If the conditions given by Eqs. 8 and 9 are satisfied, the robot must take a step on the second slope. In this case, we need to determine the leg angle  $\alpha$  which will stop the robot at the vertically upright configuration at the end of the stepping.

We first check the geometrically possible range of  $\alpha$  given the initial configuration. If the minimum distance from  $r_G$  to the second slope is shorter than the spoke length  $l$ , the robot (based on the rimless wheel model) can not physically step between the two points  $P_2$  and  $P_3$  in Fig. 7(a), which are the points of intersection of the  $l$ -radius circle centered at  $r_G$  and the second slope. Another geometric limit is the case that even 90-degree  $\alpha$ , presumably the maximum leg

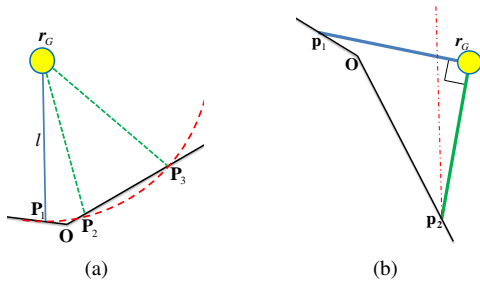


Fig. 7. Geometric limitation for the existence of GFPE: (a) The swing spoke (dotted lines) can not step between  $P_2$  and  $P_3$  because the distance between the second slope and  $r_G$  is shorter than the spoke length  $l$ . (b) The CoM would already pass the vertically upright position when the wheel with 90 degree leg angle takes a step on the second slope.

angle, cannot stop toppling as shown in Fig. 7(b). Note that in most cases we would not have these limitations since the two cases implies an extreme situation such as the slope is too steep or the robot has already fallen too much.<sup>2</sup>

For the sake of convenience, from now on we exclude the two cases in Fig. 7. If we can adjust the length of the swing spoke, which is possible for a humanoid, this limitation may be overcome in some cases. This will be considered in the future.

When the robot steps on the second slope as shown in Fig. 6(b), the angle  $\theta$  between the support spokes and the vertical line are:

$$\begin{aligned}\theta(t^-) &= \alpha - \beta \\ \theta(t^+) &= \alpha + \beta.\end{aligned}\quad (10)$$

The distance from  $O$  to the stepping point,  $P_2$  in Fig. 6(b) can be computed as:

$$d_2 = -d_1 \cos(\gamma_1 + \gamma_2) + \sqrt{4l^2 \sin^2 \alpha - d_1^2 \sin^2(\gamma_1 + \gamma_2)}, \quad (11)$$

and  $\beta$  is given as:

$$\begin{aligned}\cos \beta &= \frac{d_1 \cos \gamma_1 + d_2 \cos \gamma_2}{2l \sin \alpha} \\ \sin \beta &= \frac{-d_1 \sin \gamma_1 + d_2 \sin \gamma_2}{2l \sin \alpha}.\end{aligned}\quad (12)$$

Note that  $d_2$  and  $\beta$  are functions of  $\alpha$  only.

After the step, we expect the rimless wheel to completely stop at the top as in the right of Fig. 5(a). By virtue of conservation of energy between the third and fourth phases of Fig. 5(a),  $\dot{\theta}(t^+)$  can be obtained as follows:

$$\dot{\theta}(t^+) = \pm \sqrt{\frac{2mgl}{I_p} [1 - \cos(\alpha + \beta)]}. \quad (13)$$

<sup>2</sup>In Fig. 7(a), even if the GFPE does not exist because of this geometrical limitation, stepping on the farther boundary  $P_3$  guarantees that a rimless wheel will not topple forward after stepping at least. That is because non-existence of the point implies that stepping on  $P_2$  makes the robot topple forward and stepping on  $P_3$  can not bring the CoM to the vertically upright configuration.

Combining Eqs. 6, 4 and 13, we get the following equation:

$$\cos(2\alpha) \sqrt{\frac{2}{I_p} (E - mgl \cos \alpha)} = \sqrt{\frac{2mgl}{I_p} [1 - \cos(\alpha + \beta)]}. \quad (14)$$

Solving this equation numerically gives the leg angle  $\alpha$  and corresponding stepping point.<sup>3</sup>

The physical limitation of a humanoid implies the boundary conditions for  $\alpha$  as:

$$0 < \alpha < \frac{\pi}{4}. \quad (15)$$

*Theorem 1:* In the first scenario of Fig. 5,  $\alpha$  for the GFPE always exists between  $\alpha_o$  and  $\pi/4$ .

*Proof:* Equation 14 is continuous in  $\alpha$ . For  $\alpha = \alpha_o$ , the left terms of Equation 14 are strictly positive since Equation 9 holds. (Note that  $\beta = -\gamma_1$  when  $\alpha = \alpha_o$ .) For  $\alpha = \pi/4$ , it is strictly negative. Therefore, at least one  $\alpha$  between  $\alpha_o$  and  $\pi/4$  satisfies Equation 14.

The proof might sound counter-intuitive since one can ask if there is any case the robot topples again after taking the step because of large initial disturbance. The reason is that the rimless wheel model completely stops at the moment of the step where  $\alpha = \pi/4$ , which yields the zero angular velocity in Eq. 6 regardless of the magnitude of  $E$ . This result comes from no slip condition and the inelastic collision model. In practice, if the initial disturbance is very large, a robot may experience slippage and the conservation of angular momentum during inelastic collision may not be realistic.

*Theorem 2:* The solution  $\alpha$  is unique.

*Proof:* We prove this by showing that the total energy after the impact  $E^+(\alpha)$  monotonically decreases with increasing  $\alpha$ . Since the solution should satisfy  $E^+(\alpha) = mgl$ , there should be only one  $\alpha$  for the energy. Given  $\alpha_1$  and  $\alpha_2$  where  $\alpha_2 > \alpha_1$ , let  $E^+(\alpha_1)$  and  $E^+(\alpha_2)$  be the total energies after the impact. The energy difference can be computed as following:

$$E^+(\alpha_2) - E^+(\alpha_1) = mgl(\cos \alpha_2 - \cos \alpha_1)(1 - \cos^2(2\alpha_2)), \quad (16)$$

which is strictly negative when  $\alpha_2 > \alpha_1$  and  $\alpha \in [0, \frac{\pi}{4}]$ . Extension of this proof to the non-level ground is trivial when a solution exists.

#### D. Duration of step

In an urgent situation like reactive stepping, the duration of stepping is a critical parameter for the stepping controller. One of the benefits from using the GFPE is that we can estimate the time during which the robot can take a step. For example, in the capture point approach, the point should be stepped on by the robot at the exact moment it is computed [8]. However, the robot must have dynamics and stepping motion takes a certain amount of time, by which the capture point may displace.

<sup>3</sup>We use  $\cos(\alpha + \beta) = \cos \alpha \cos \beta - \sin \alpha \sin \beta$ .

In addition, the duration of stepping is very important also for the high-level controller. If the estimated duration of step is too short for the robot to physically take a step, the high-level controller may want to switch to an emergency controller such as fall-avoidance or damage minimization from fall, instead of trying to take a step.

Since we model a humanoid as a 2D inverted pendulum, an incomplete elliptic integral of the first kind is used to obtain the duration [17].

### E. Comparison with Capture Point

The capture point was proposed as an instantaneous point on the ground where a humanoid should step on at the moment it is computed in order to come to a complete stop with CoM directly above the CoP [8]. The capture point is state-dependent and therefore by the time the robot takes a step, the point may move away. Therefore in practice, the capture point has to be tracked and estimated multiple times during stepping, and the controller may need to modify the leg trajectory accordingly.

Another practical issue with the capture point is that its location does not always work well as a trigger to start the controller. For example, there are cases where although the robot has already fallen significantly, the capture point barely exited the support area, which can be the trigger to take a step. An early trigger time is very critical for reactive stepping control to succeed because the controller typically has a very limited time for stepping.<sup>4</sup> In other words, even if we knew that the robot must take a step because of instability, capture point might be still too close to the feet to step on it. (See the blue cross at the front end of the feet in Fig. 9(b).)

On the other hand, the GFPE is predictive; it yields a future stepping point and duration for the step. Therefore, with a perfect 2D inverted pendulum model, capture point approaches the GFPE as in Fig. 8. We can clearly see capture point lags behind our step point since it is instantaneous. The sharp change of capture point is caused by the collision of the swing spoke since the rimless wheel loses some energy at that moment. Integrating the dynamic equation to estimate the future capture point may help, however, that requires the computational burden.

In addition, the GFPE exists on the non-level ground as long as the slopes change discretely, whereas we should assume a flat ground for the capture point so that a robot can perform the linear inverted pendulum motion.

## IV. SIMULATION

The reactive stepping controller has been implemented in our *Locomote* software package based on Webots [12]. The robot in our simulation has two legs with 6-dof each, is 1.3 m tall and weighs 55 kg. The simulator checks the maximum joint angle/torque of each joint as well as self-collision.

<sup>4</sup>A forward fall of an adult takes about 0.98 second starting from a 15° inclination [18].

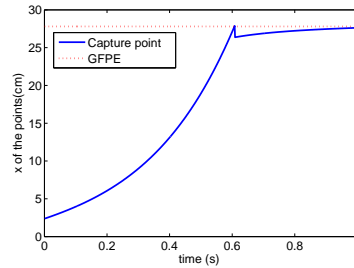


Fig. 8. Comparison between capture point and the FPE. The graph is generated by a simulation of a 2D rimless wheel.  $l = 0.6m$ ,  $\theta(0) = 5.7deg$  and  $\dot{\theta}(0) = 32deg/sec$  are used, which corresponds to the simulation of Fig. 9.

### A. Step trigger

A simple step trigger has been implemented to make a decision of whether to take a step or not. Until the trigger turns on, the momentum controller is supposed to respect linear momentum to recover balance by postural motion without stepping. The trigger also uses the GFPE. If the GFPE moves out of the support area, we consider the robot should take a step and switch to the reactive stepping controller from the postural balance controller. This switch can happen anytime; after the follow-up step, the controller returns to the postural balance controller.

We have used  $\Gamma_{11} = \text{diag}\{5, 5, 5\}$ ,  $\Gamma_{21} = \text{diag}\{40, 20, 40\}$  and  $\Gamma_{22} = \text{diag}\{8, 3, 8\}$  for the gains for the postural balance controller. For the reactive stepping controller, we have used  $\Gamma_{11} = \text{diag}\{20, 20, 20\}$ ,  $\Gamma_{21} = \text{diag}\{2, 2, 5\}$  and  $\Gamma_{22} = \text{diag}\{3, 3, 8\}$ .

### B. Trajectories of the CoM and swing foot for stepping

Given a GFPE location, we design trajectories of the CoM and the swing foot. The CoM trajectory is a reference for the rate change of linear momentum (Eq. 2), and the swing foot trajectory is one of the optimization goals in the momentum controller (See [1]). In this paper we only use the right leg for stepping. (In the future, an algorithm for choosing a swing leg will be considered.)

Each trajectory is a quadratic Bezier curve.<sup>5</sup> As in [19], the planar CoM trajectory uses current CoM  $r_G$ , pivot foot position  $T_l$  and the half-way between the pivot foot and the target stepping point  $\frac{T_l + T_t}{2}$ . The reason for using the center of the pivot foot is we want the CoP to move inside of the pivot foot print so that a robot can make a stable step. The height of CoM trajectory can be designed by modeling a robot as a rimless wheel model on the slope. The swing foot trajectory uses  $T_r$ , slightly lifted  $T_r$  and  $T_t$ . For smooth motion, velocities of the trajectories are parameterized so that it has zero velocity at the start and the end. The duration of the trajectory comes from the duration of stepping multiplied by a heuristic safety factor (70%)

<sup>5</sup>A quadratic Bezier curve is defined as:

$$T = (1-t)^2 T_0 + 2(1-t)t T_1 + t^2 T_2, t \in [0, 1]$$

considering the discrepancy between the simplified model and the real humanoid.

### C. Reactive stepping

By switching the control gains for the rate changes of momenta, the reactive stepping controller has been implemented for push recovery. Figs. 9 and 10 show snapshots of the simulation results where the robot reactively steps on a 11.5 degree uphill and 6 degree downhill, respectively, after a 220 N push from behind applied for 0.1 sec to the center of the body. The CoM height is 0.6m when the robot is pushed.

The reactive stepping controller starts after the application of the push. For the robot to follow the rimless wheel model, the robot takes a follow-up step with the left leg. The GFPE is shown as a red cross on the slope. Note that capture point is still around the base convex hull (Fig. 9(b)) when the stepping point on the slope clearly shows the necessity of reactive stepping.

When the same push is applied to the robot with the postural balance controller, the robot fails to take a step because it sacrifices angular momentum too much which must accompany large change of the upper body orientation. The controller tries to keep the CoM close to the reference trajectory and causes the bending motion of the upper body, which results in joint limit violation of the hip. Note that we use the exactly same trajectories for the postural balance controller (linear momentum respecting) and the reactive stepping controller (angular momentum respecting).

Fig. 11 shows the rate changes of linear and angular momentum (control inputs) from the simulations by the postural balance controller and the reactive stepping controller. In the lower left of Fig. 11, the large gap between the desired rate change of angular momentum and the admissible rate change shows that the postural balance controller tries to track the linear momentum by sacrificing precise control of the angular momentum. On the other hand, in the right of Fig. 11, the reactive stepping controller generates the admissible rate change of angular momentum which is closer to the desired rate, by allowing the tracking error of the linear momentum.

Various magnitude of pushes have been applied from behind within a 30 degree cone, and the robot can successfully take a reactive step according to the pushes. A push to the side or backward is not well handled because of complicated reasons such as the asymmetric configuration of the robot. This will be considered in the future.

In our simulations on the flat ground, the proposed reactive stepping controller can survive up to a 280 N push for 0.1 sec from behind, while the postural balance controller *without* stepping cannot recover balance for forces larger than a 180 N push for 0.1 sec.

## V. CONCLUSION

We have presented a unified framework for push recovery on level and non-level grounds using momentum-based balance control and reactive stepping. By switching between controllers for respecting linear momentum and angular momentum, a biped robot can choose to take a step or re-balance

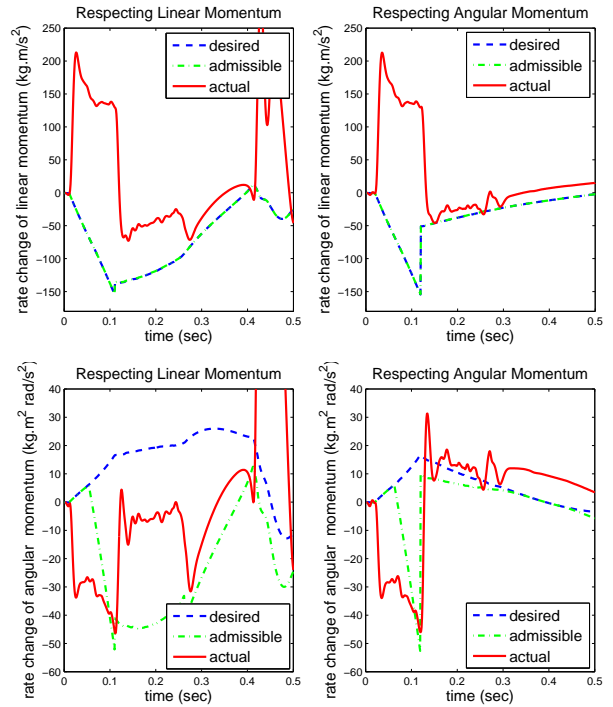


Fig. 11. Desired and actual rate changes of momenta from simulations with the two momentum controllers: (RIGHT) respecting linear momentum and (LEFT) respecting angular momentum (Fig. 9). X component of linear momentum and Z component of angular momentum are shown, where Y-axis is the vertical axis. A 220 N push for 0.1 sec is applied to the robot from behind in both cases.

without stepping according to the magnitude of external disturbance. The foot placement estimator (FPE) has been exploited and extended for stepping on non-level ground, and has been renamed as the generalized FPE, GFPE. Desirable properties of GFPE includes: 1) GFPE is predictive so that the controller may start stepping early. 2) GFPE may exist on the non-level ground while many previously proposed reference points for stepping do not. 3) Computation of GFPE yields both the time required for stepping as well as the location of the point itself. The derivation and analysis of the GFPE on non-level ground have been introduced, and we compared it to capture point. The controller has been implemented on a full sized humanoid for dynamic continuous stepping on the flat surface and reactive stepping on a slope. In the simulations, switching from respecting linear momentum to angular momentum yielded smooth reactive stepping.

Since there has been no quantitative measure for performance of balance controllers and reactive stepping controllers, dimensionless analysis may be required in the future. As a test case, we are implementing the proposed controller on a small humanoid hardware. Also the decision-making algorithm for taking a reactive step given the current states of a robot will be re-visited.

## VI. ACKNOWLEDGMENTS

We are grateful to Prof. Sung-Hee Lee of GIST, Korea for significant and fruitful discussion.

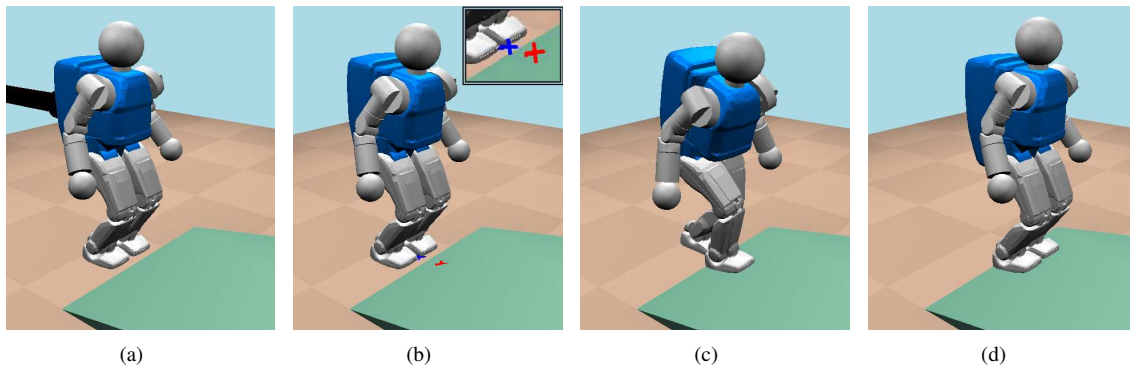


Fig. 9. Snapshots of reactive stepping on a 11.5 degree uphill. (a) The robot gets a push (shown by the black line) on the backpack. The magnitude of the push is 220N for a duration of 0.1 sec. (b) GFPE (red cross) and capture point (blue cross) are shown. capture point is still close to the feet. The magnified view of the points is shown in the upper right. (c) The robot is stepping on the GFPE. (d) The robot has been balanced after the follow step.

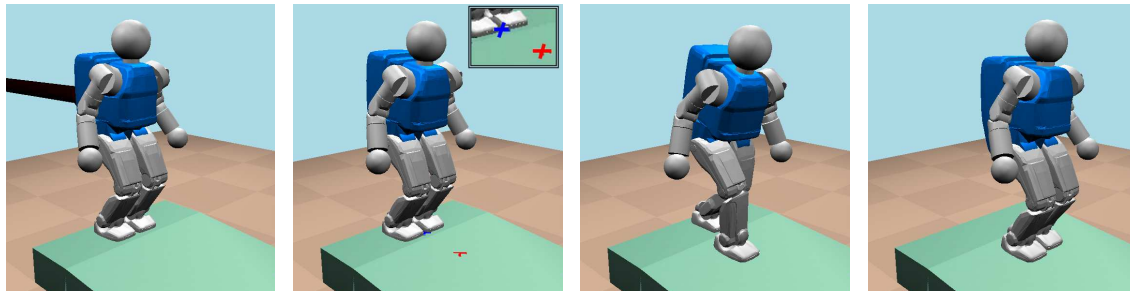


Fig. 10. Snapshots of reactive stepping on a 6 degree downhill. The red cross shows the location of the GFPE. Note that the capture point (blue cross) has barely existed the footprint.

## REFERENCES

- [1] S.-H. Lee and A. Goswami, "Ground reaction force control at each foot: A momentum-based humanoid balance controller for non-level and non-stationary ground," in *IEEE/RSJ Int'l Conf. on Intelligent Robots and Systems (IROS)*, Taipei, Taiwan, Oct 2010, pp. 3157–3162.
- [2] S. Kudoh, T. Komura, and K. Ikeuchi, "The dynamic postural adjustment with the quadratic programming method," in *IEEE/RSJ Int'l Conf. on Intelligent Robots and Systems (IROS)*, EPFL, Switzerland, Sep 2002, pp. 2563 – 2568.
- [3] S. Kagami, F. Kanehiro, Y. Tamiya, M. Inaba, and H. Inoue, "AutoBalancer: An online dynamic balance compensation scheme for humanoid robots," in *Proc. of the 4th Inter. Workshop on Algorithmic Foundation on Robotics*, 2000.
- [4] S. Kajita, F. Kanehiro, K. Kaneko, K. Fujiwara, K. Harada, K. Yokoi, and H. Hirukawa, "Resolved momentum control: Humanoid motion planning based on the linear and angular momentum," in *IEEE/RSJ Int'l Conf. on Intelligent Robots and Systems (IROS)*, vol. 2, 2003, Las Vegas, NV, USA, pp. 1644–1650.
- [5] A. Hofmann, M. Popovic, and H. Herr, "Exploiting angular momentum to enhance bipedal center-of-mass control," in *IEEE Int'l Conf. on Robotics and Automation (ICRA)*, Kobe, Japan, May 2009, pp. 4423–4429.
- [6] A. Macchietto, V. Zordan, and C. R. Shelton, "Momentum control for balance," *ACM Transactions on Graphics*, vol. 28, no. 3, pp. 80:1–80:8, July 2009.
- [7] D. Wight, E. Kubica, and D. Wang, "Introduction of the foot placement estimator: A dynamic measure of balance for bipedal robotics," *Journal of Computational and Nonlinear Dynamics*, vol. 3, 2008.
- [8] J. Pratt, J. Carff, S. Drakunov, and A. Goswami, "Capture point: A step toward humanoid push recovery," in *6th IEEE-RAS International Conference on Humanoid Robots*, December, Genoa, Italy 2006, pp. 200 – 207.
- [9] A. L. Hof, "The extrapolated center of mass concept suggests a simple control of balance in walking," *Human Movement Science*, vol. 27, no. 1, pp. 112 – 125, 2008.
- [10] Z. Aftab, T. Robert, and P.-B. Wieber, "Comparison of Capture Point estimation with human foot placement : Applicability and Limitations," in *5èmes Journées Nationales de la Robotique Humanoïde*, Poitiers France, 06 2010, Cluster de recherche, Région Rhone-Alpes.
- [11] B.-K. Cho and J.-H. Oh, "Practical experiment of balancing for a hopping humanoid biped against various disturbance," in *IEEE/RSJ Int'l Conf. on Intelligent Robots and Systems (IROS)*, Taipei, Taiwan, 2010, pp. 4464–4470.
- [12] O. Michel, "Webots: Professional mobile robot simulation," *International Journal of Advanced Robotic Systems*, vol. 1, no. 1, pp. 39–42, 2004.
- [13] M. Millard, D. Wight, J. McPhee, E. Kubica, and D. Wang, "Human foot placement and balance in the sagittal plane," *J Biomech Eng*, vol. 131, no. 12, p. 121001, 2009. [Online]. Available: <http://www.biomedsearch.com/nih/Human-foot-placement-balance-in/20524724.html>
- [14] M. Morisawa, F. Kanehiro, K. Kaneko, N. Mansard, J. Sola, E. Yoshida, K. Yokoi, and J.-P. Laumond, "Combining suppression of the disturbance and reactive stepping for recovering balance," in *IEEE/RSJ Int'l Conf. on Intelligent Robots and Systems (IROS)*, Taipei, Taiwan, 2010, pp. 3150–3156.
- [15] A. Goswami, "Postural stability of biped robots and the foot rotation indicator (FRI) point," *Int'l J. of Robotics Research*, vol. 18, no. 6, pp. 523–533, 1999.
- [16] M. J. Coleman, A. Chatterjee, and A. Ruina, "Motions of a rimless spoked wheel: a simple 3d system with impacts," *Dynamics and Stability of Systems*, vol. 12, no. 3, pp. 139–160, 2008.
- [17] S.-K. Yun, A. Goswami, and Y. Sakagami, "Safe fall: Humanoid robot fall direction change through intelligent stepping and inertia shaping," in *IEEE Int'l Conf. on Robotics and Automation (ICRA)*, May 2009, pp. 781–787.
- [18] J.-S. Tan, J. J. Eng, S. R. Robinovitch, and B. Warnick, "Wrist impact velocities are smaller in forward falls than backward falls from standing," vol. 39, no. 10, pp. 1804–1811, 2006.
- [19] C.-C. Wu and V. Zordan, "Goal-directed stepping with momentum control," in *ACM SIGGRAPH/Eurographics Symposium on Computer Animation (SCA)*, Madrid, Spain, July 2010.